ANL-HEP-TR--92-97

DE93 002783

SDC
SOLENOIDAL DETECTOR NOTES

Effect of Pb and Air Absorber Thickness on ^{137}Cs Signal

D. Jankowski, D. Lopiano, and R. Stanek
High Energy Physics Division
Argonne National Laboratory, Argonne, Illinois 60439

22 October 1992

SDC-92-350
ANL-HEP-TR-92-97

Effect of Pb and Air Absorber Thickness on ^{137}Cs Signal

D. Jankowski, D. Lopiano and R. Stanek
Argonne National Laboratory
9700 S. Cass Ave.
Argonne, Il 60439

1 Abstract

We present the results of a measurement to understand the effects of transverse misplacement of the ^{137}Cs source tube inside the cast Pb plates of the SDC EMC calorimeter. The PMT current from a scintillator was measured as the ^{137}Cs source was displaced by varying thicknesses of Pb, as well as varying thicknesses of air gap. At a nominal depth of 2 mm in Pb, we find a change in scintillator output of about 25%/mm, and about 10%/mm of air gap. The data are compared to a simple calculation. By taking the sum of the scintillators on top and below a source tube, we estimate a source tube displacement of $\pm 450\mu$ will cause an error in the PMT output by 1%.

2 Introduction

In the ANL design for the cast Pb EMC of the BCAL[1], the source tubes are embedded in the Pb absorber, and are constrained between towers at the bulkheads. If a low energy source such as ^{137}Cs is used to measure the response of a scintillator tile, the tolerance of the source tube placement in the Pb perpendicular to the scintillator becomes an important issue due to varying amounts of Pb between the scintillator and source. Furthermore, if

[1]SDC Technical Proposal. SDC-92-201

* Work supported by the U.S. Department of Energy, Division of High Energy Physics, Contract W-31-109-ENG-38.

the scintillator varies in the distance away from the Pb layer containing the source tube, this air gap can also cause miscalibrations due to a change in solid angle subtended.

We have measured these effects by running a source over a piece of scintillator and varying the amount of absorber between the source and the scintillator. The absorber was of two types: Pb sheets with grooves machined to precise thicknesses, and ordinary cardboard to approximate an air gap.

3 Description of Measurement

Figures 1a and 1b show a diagram of the test setup. Inside a light-tight box we placed a piece of 10cm x 10cm x 2.5mm Kuraray SCSN-81 plastic scintillator coupled in the standard fashion with Y7 waveshifter to a Hamamatsu R580 phototube. Depending on the measurement, either a thickness of Pb or a thickness of cardboard was placed on the surface of the scintillator. A 2 mCi ^{137}Cs source was driven through a source tube across the top of the absorber. The thickness of Pb absorber was varied to simulate the source tube at varying depths in the proposed cast Pb plate, and the thickness of cardboard was varied to simulate varying distances of the scintillator from the cast plate. The output of the PMT was coupled into a CAMAC multiplexed ADC and the current integrated for 20 msec and read out by an IBM XT.

The Pb absorbers consisted of a series of 12 mm thick Pb plates, 25cm x 15cm, each with a groove machined to accomodate the source tube. The Pb remaining in the groove varied in thickness between 0.5 mm and 3.0 mm. See Figure 1a. An air gap was simulated by stacking varying layers of cardboard between the scintillator, and a piece of 1.6 mm G-10 which supported the source tube. The G-10 had the benefit of absorbing low energy βs. The cardboard varied in thickness between 0 mm and 7.3 mm. See Figure 1b.

The PMT HV was such that the minimum absorber gave currents of about 75% of ADC saturation. The source was driven from it's garage into the test assembly, and the PMT current was recorded on disk as the source was in motion. This procedure was performed three times for each absorber thickness.

4 Results

Figure 2 shows a typical source scan for each of three measurements. The asymmetric baseline at large times is due to the source being not in motion near the end of the scintillator. The mean PMT current is calculated by taking the average of the center bin in the peak and ± 10 bins either side of it. A pedestal value measured at the beginning of each scan is subtracted, and the 3 measurement values were averaged.

Figures 3a-b show the variation of the source intensity as the amount of Pb attenuator is varied. The difference between figures 3a and 3b is basically a broken then repaired optical fiber. The dotted curves are the expected yield according to the Appendix using an attenuation length of $\lambda = 7.93$ mm. The curves are normalized to the data at 2.5 mm.

Figure 4 shows the variation of the source intensity as the distance from the source to scintillator is varied with cardboard attenuator. Again, the dotted curves are the result of Eq. 5 with $\lambda = 171.4$ mm. Note that air has an attenuation length of about 10^5 mm.

5 Conclusion

We see from the Pb data that, at the nominal 2 mm depth, a variation of 1 mm causes a 25% change in the intensity on a single scintillator tile. Also we see that the cardboard data shows about a 10% change per mm at the 2 mm point.

Using the calculated values of intensities for the Pb absorber, we can add together the intensities of two scintillators on either side of a Pb plate containing the source tube. We see from Figure 5 that summing the top and bottom scintillators give much more immunity to source misalignment. A 1% change occurs if the source tube is displaced by ± 0.45 mm.

6 Appendix

Consider the problem of a point source and an infinite plane a distance s away (see figure 6), the expression for the intensity I as a function on position on the plane is given by ,

$$dI = I_o e^{-\frac{r}{\lambda}} d\Omega$$

where

$$d\Omega = \frac{\vec{r} \cdot \hat{n} da}{r^3}$$

$$= \frac{r \cos\theta dx dy}{r^3}$$

$$= \frac{s dx dy}{\sqrt{x^2 + y^2 + s^2}^3}$$

Neglecting rescattering into the scintillator,

$$\frac{I}{I_o} = s \int_0^L dy \int_0^W dx \frac{e^{-\frac{\sqrt{s^2+x^2+y^2}}{\lambda}}}{\sqrt{s^2 + x^2 + y^2}^3} \tag{1}$$

Recasting this in plane-polar coordinates, $x = rcos\phi$, $y = rsin\phi$, $dxdy = rdrd\phi$, results in an integral of the form

$$\frac{I}{I_o} = s \int_0^{\frac{\pi}{2}} d\phi \int_0^{P(L,W,\phi)} rdr \frac{e^{-\frac{\sqrt{s^2+r^2}}{\lambda}}}{\sqrt{s^2 + r^2}^3} \tag{2}$$

where

$$P(L, W, \phi) = \sqrt{W^2 + L \tan^2 \phi} \; for \; \phi \leq \arctan \frac{L}{W}$$

$$= \sqrt{L^2 + W \cot^2 \phi} \; for \; \phi \geq \arctan \frac{L}{W}$$

Now performing a change of variable $\alpha^2 = s^2 + r^2$, $d\alpha = \frac{rdr}{\sqrt{s^2+r^2}}$, the integral becomes

$$\frac{I}{I_o} = s \int_0^{\frac{\pi}{2}} d\phi \int_s^{Q(s,L,W,\phi)} d\alpha \frac{e^{-\frac{\alpha}{\lambda}}}{\alpha^2} \tag{3}$$

where

$$Q(s, L, W, \phi) = \sqrt{s^2 + P(L, W, \phi)^2}$$

Eq. 3 can be expressed in terms of the expontential integral function Ei(x),

$$\frac{I}{I_o} = s \int -\left(\frac{e^{-\frac{\alpha}{\lambda}}}{\alpha} + \frac{1}{\lambda} Ei(-\frac{\alpha}{\lambda})\right)\Big|_s^{Q(s,L,W,\phi)} d\phi \tag{4}$$

The limits of integration are $x \in [0, W]$ and $y \in [0, L]$. In the modified polar variables ϕ and α, $\in [0, \frac{\pi}{2}]$ and $\alpha \in [s, Q(L, W, \theta)]$. The function Q will be bounded by $\sqrt{s^2 + L^2} \leq Q(s, L, W, \theta) \leq \sqrt{s^2 + L^2 + W^2}$. For $L = 100$ and $W = 100$ the above expression reduces to

$$\frac{I}{I_o} = \frac{\pi}{2} s(\frac{e^{-\frac{s}{\lambda}}}{s} + \frac{1}{\lambda} Ei(-\frac{s}{\lambda})) \tag{5}$$

by noting that both terms in eq. 4 go to zero for large α.

Figure Captions

Figure 1(a). A sketch of the setup for measuring the attenuation of Pb absorber. **(b).** Setup for air absorber measurement. Note the fixed attenuator of 1.6 mm G-10 always in series with the varying cardboard material.

Figure 2. Data from three consecutive source scans with identical geometry. The source is started moving and then the acquisition system is started at arbitrary times thereafter.

Figure 3(a). The mean PMT current from ^{137}Cs irradiation as a function of the depth of the source in Pb absorber. **(b).** Same as (a)but with different parameters in the phototube optics. The dotted curve is from the Appendix with λ=7.93 mm.

Figure 4. The mean PMT current from ^{137}Cs irradiation as a function of the depth of the source in cardboard absorber. The data taken always had 1.6 mm of G-10 immediately downstream of the source. The dotted curve is from the Appendix with λ=171.4 mm.

Figure 5. A calculated sum of the signal from top + bottom scintillators assuming the dotted curve in figure 3. We assume the source is varied about the 2 mm point in the Pb absorber. The dashed line shows that the sum varies no more than 1% if the source tube is misplaced by $\pm 450\mu$

Figure 6. The geometry assumed in the Appendix calculation of the scintillator response to photons through an absorber.

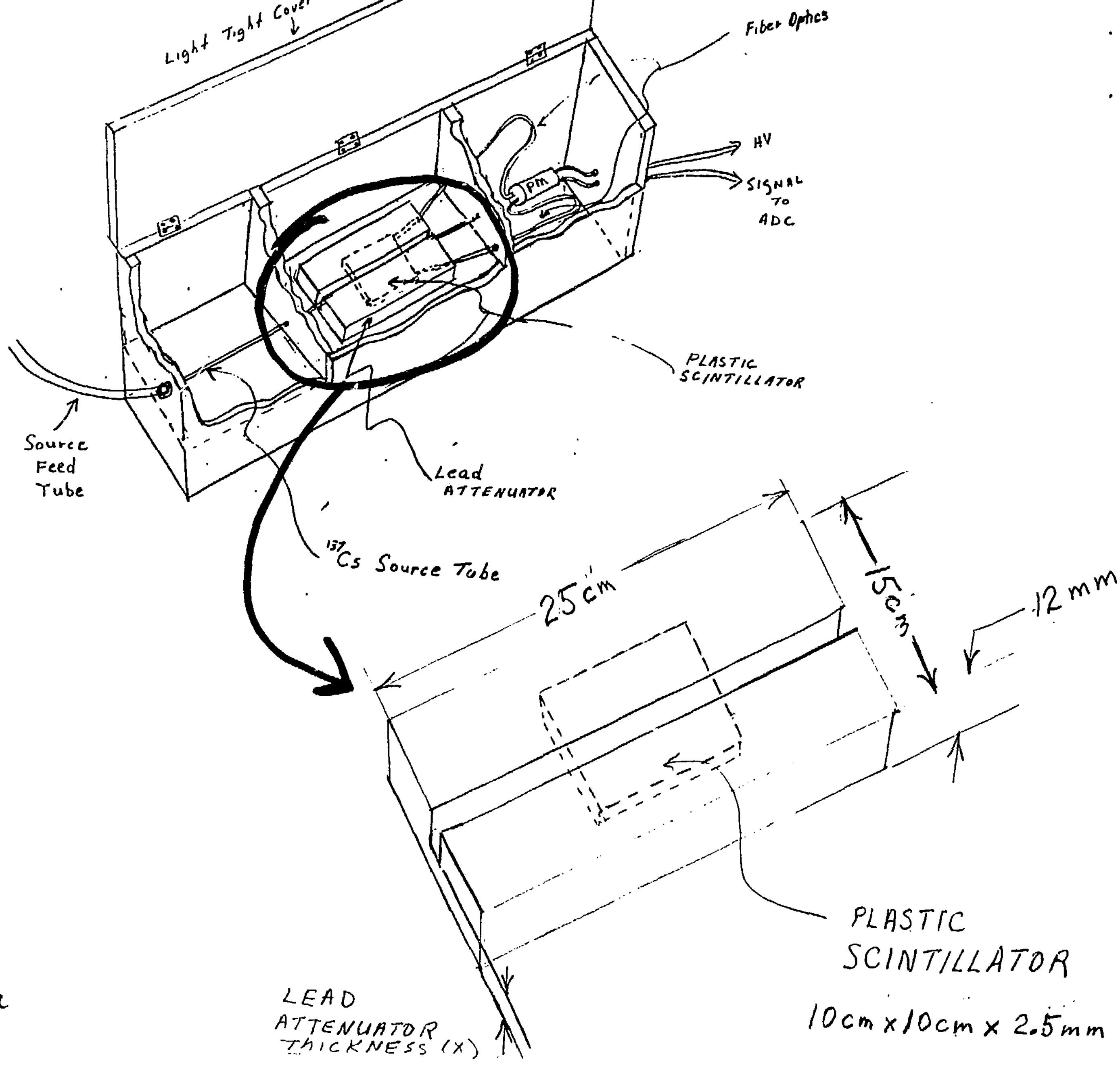

Light Tight Cover
Fiber Optics
HV
SIGNAL TO ADC
PM
PLASTIC SCINTILLATOR
Source Feed Tube
Lead ATTENUATOR
^{137}Cs Source Tube
25 cm
15 cm
12 mm
PLASTIC SCINTILLATOR
10cm x 10cm x 2.5mm
LEAD ATTENUATOR THICKNESS (X)

Fig-1a

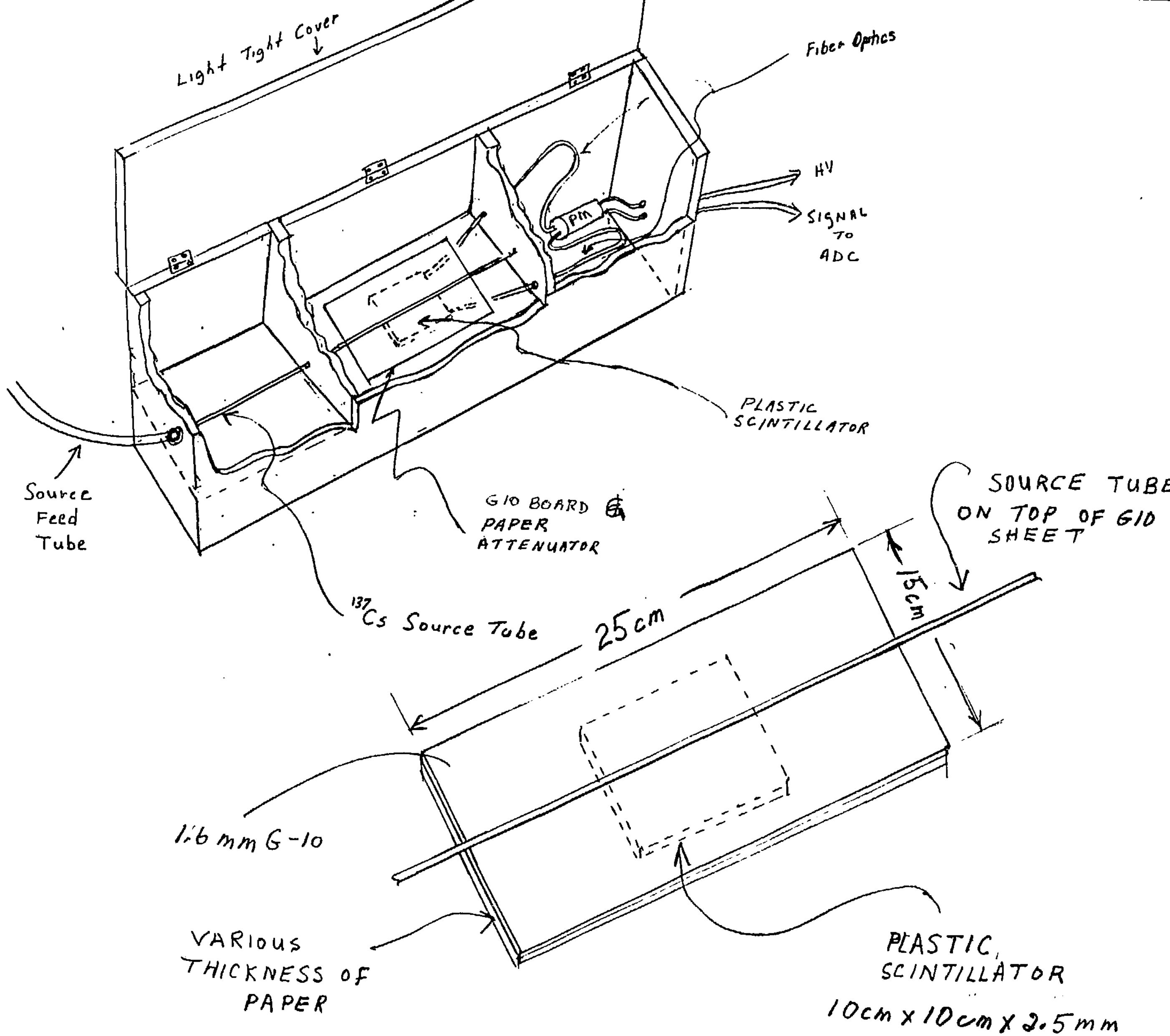
Light Tight Cover
Fiber Optics
HV
SIGNAL TO ADC
PM
PLASTIC SCINTILLATOR
Source Feed Tube
G10 BOARD & PAPER ATTENUATOR
^{137}Cs Source Tube
SOURCE TUBE ON TOP OF G10 SHEET
25cm
15cm
1.6 mm G-10
VARIOUS THICKNESS OF PAPER
PLASTIC SCINTILLATOR
10cm x 10cm x 2.5mm

Fig-1b

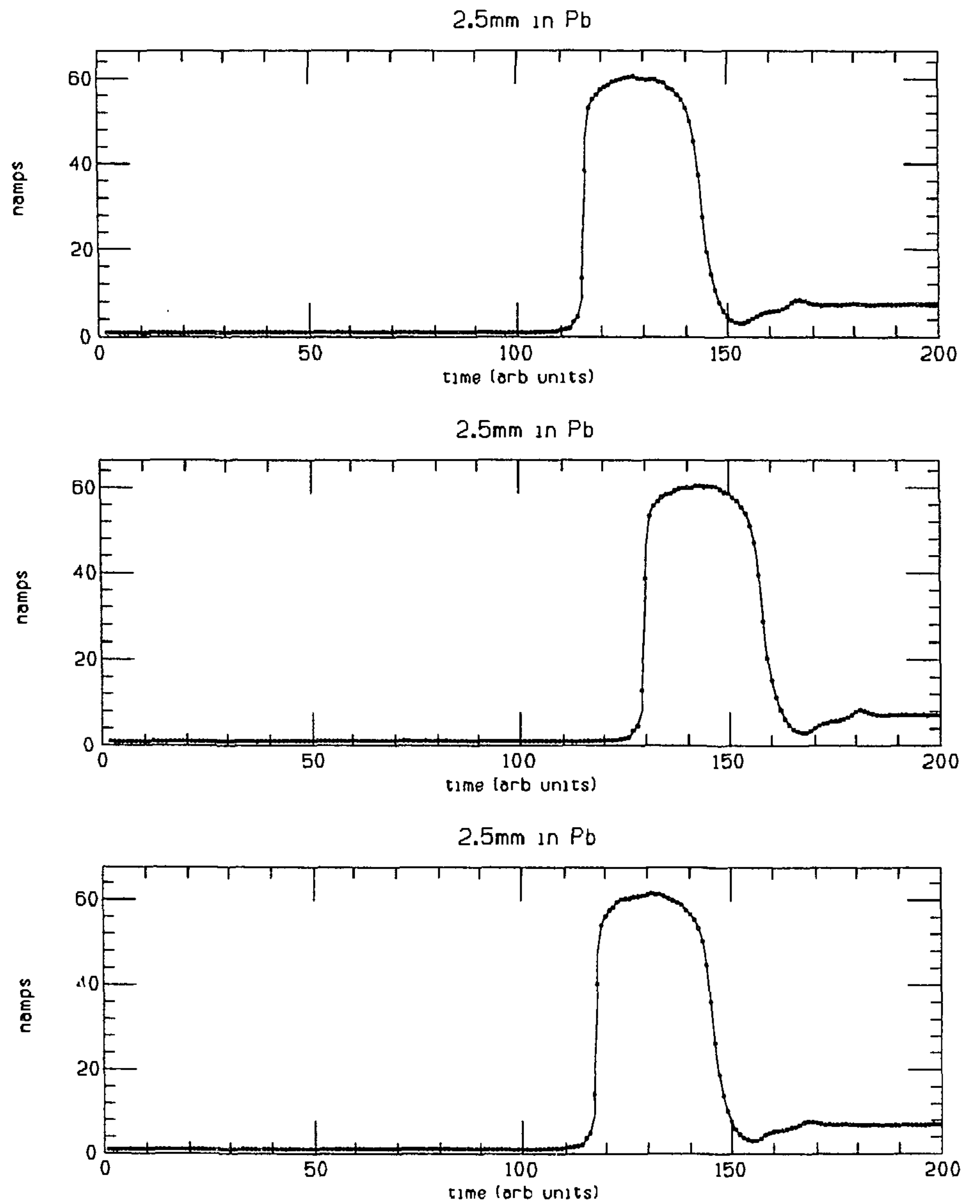
2.5mm in Pb
namps
time (arb units)
0
20
40
60
0
50
100
150
200
2.5mm in Pb
namps
time (arb units)
2.5mm in Pb
namps
time (arb units)

Fig-2

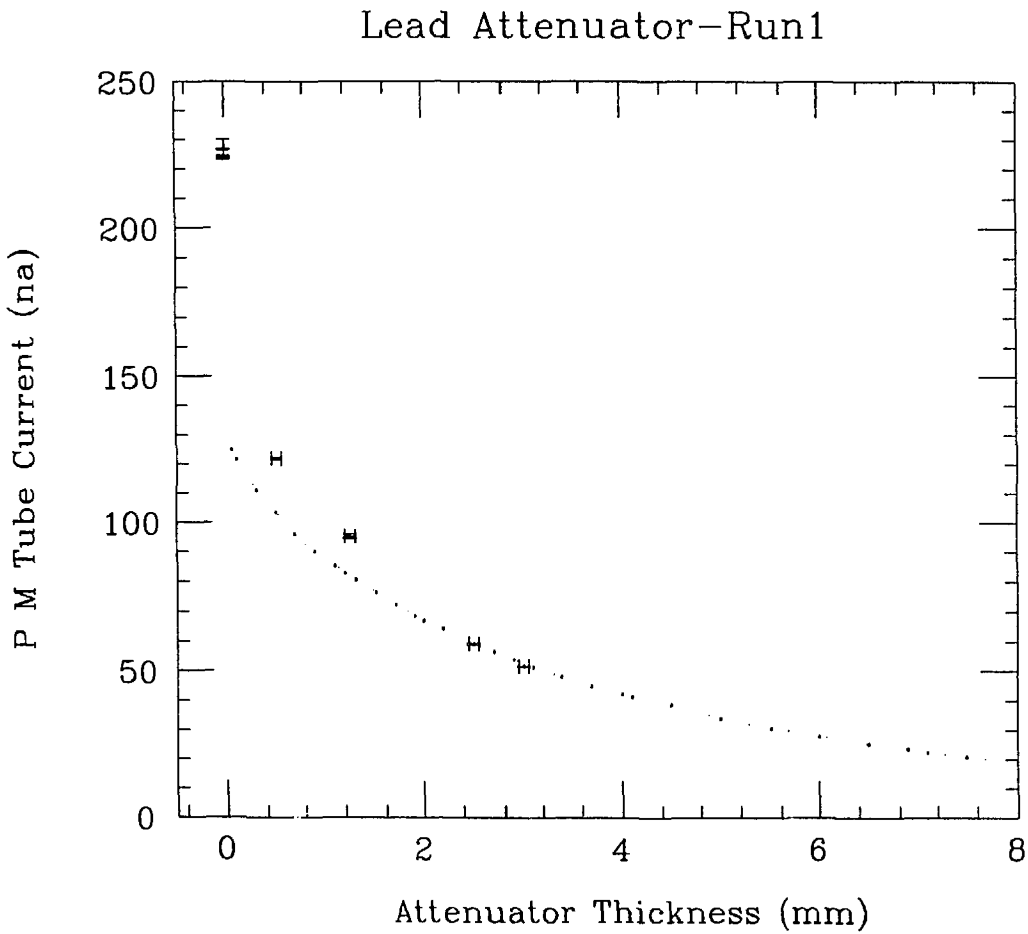

Calculated Attn. With Cs^{137}(dot curve)

Fig-3a

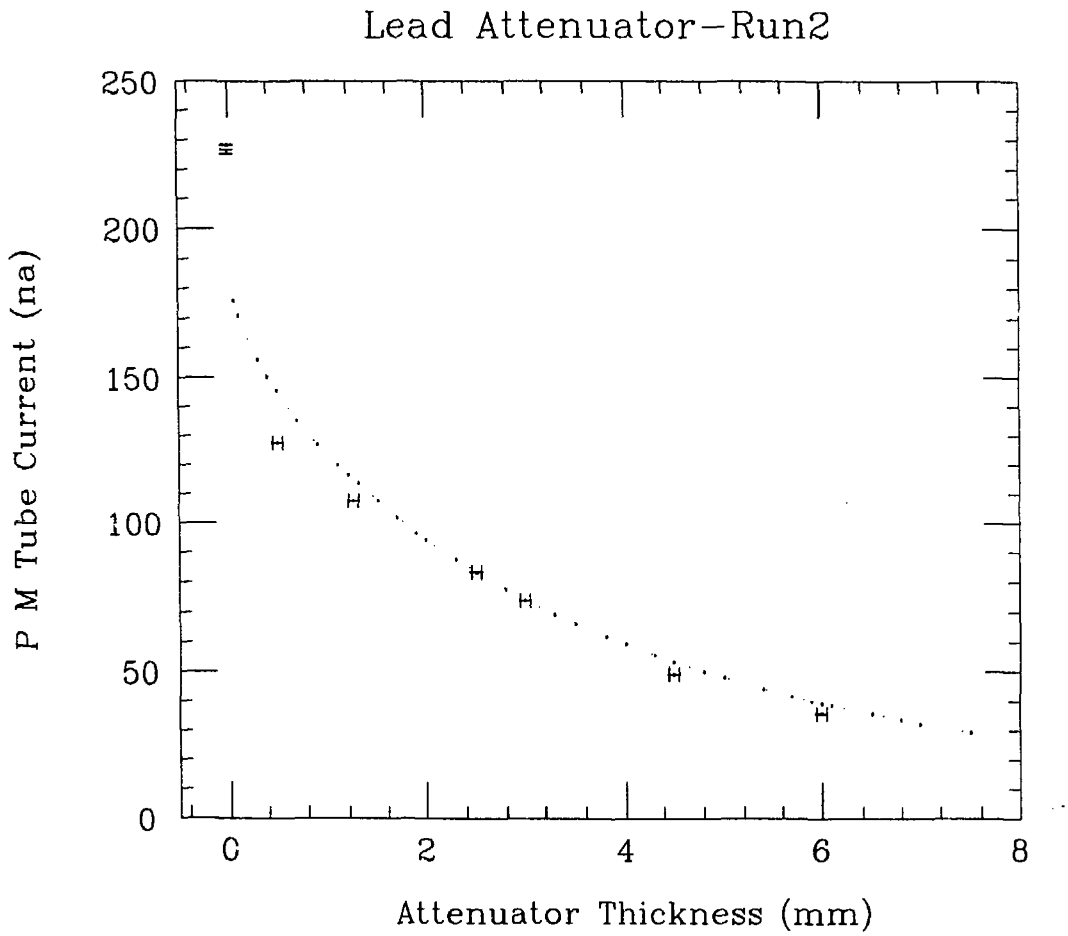

Calculated Attn. With Cs^{137} (dot curve)

Fig-3b

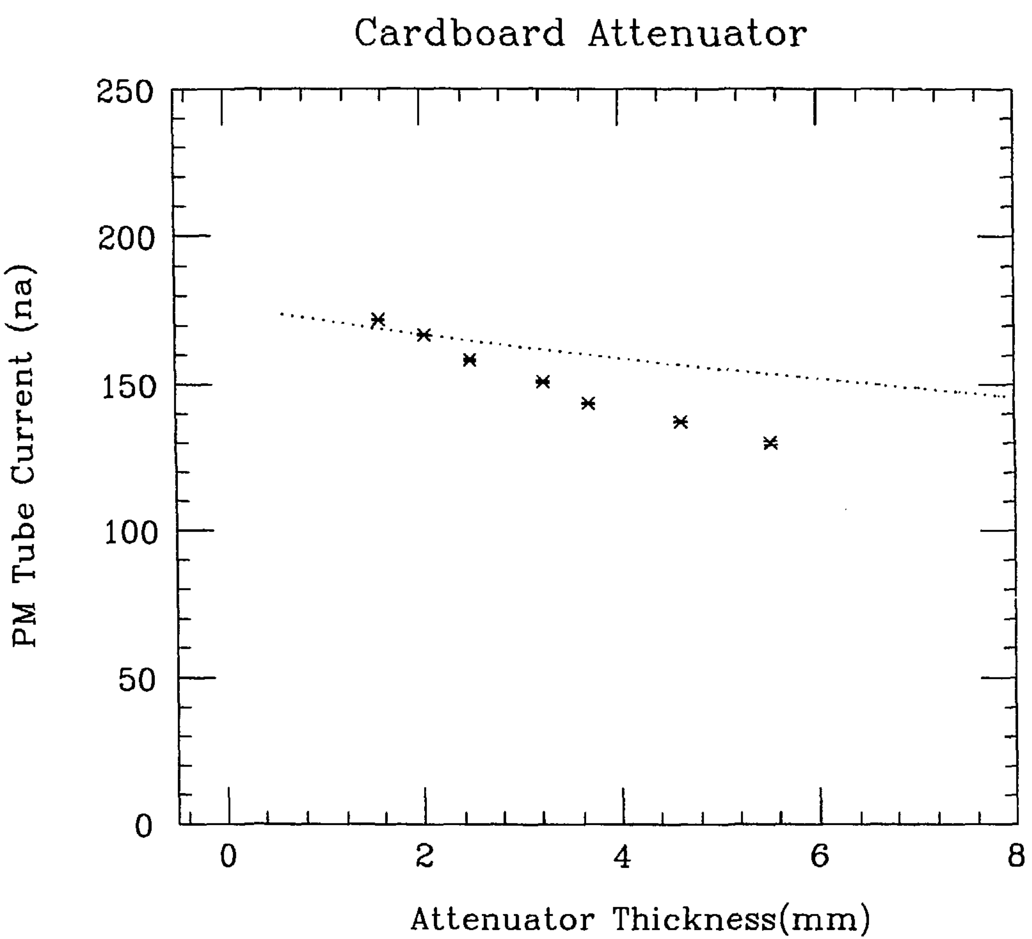

Calculated Attn. With Cs^{137} (dot curve)

Fig - 4

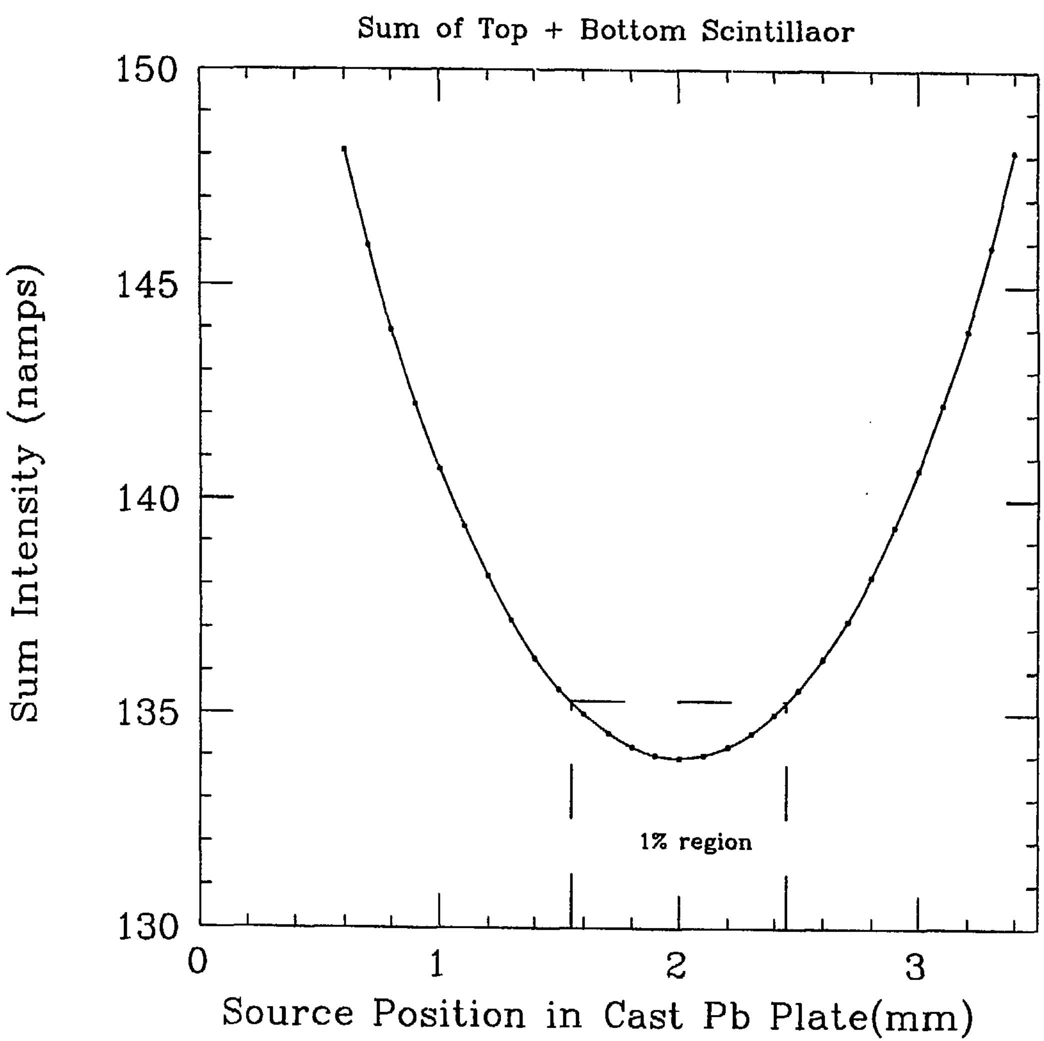
Sum of Top + Bottom Scintillaor
150
145
140
135
130
0
1
2
3
Sum Intensity (namps)
Source Position in Cast Pb Plate(mm)
1% region

Fig-5

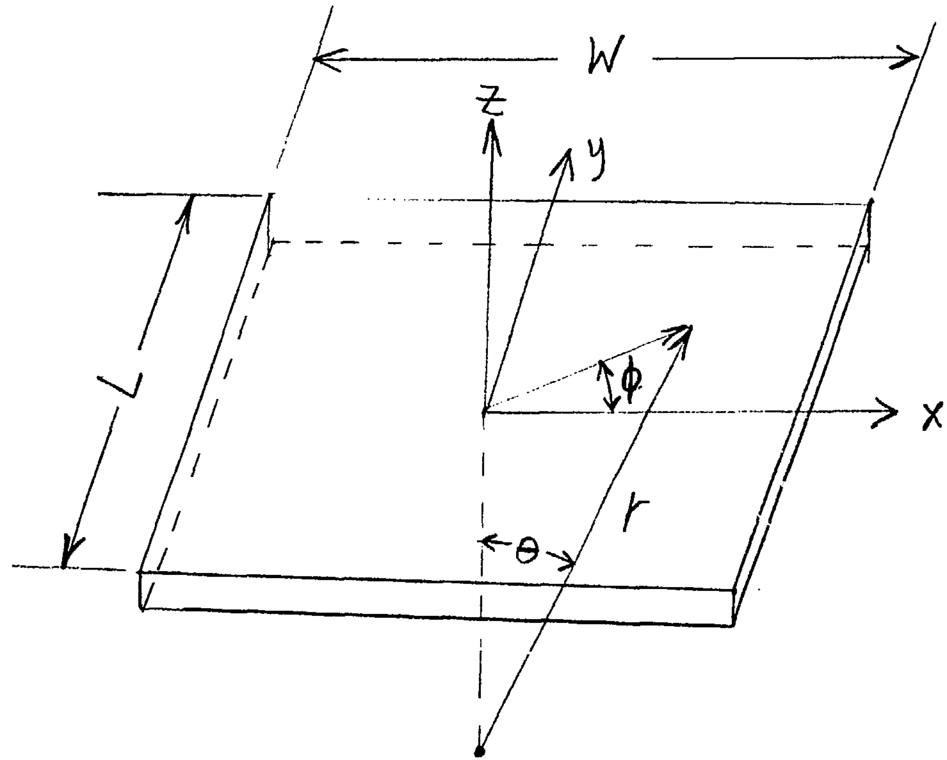

Fig-6